Modeling of Leachate Characteristics and Clogging of Gravel Drainage Mesocosms Permeated with Landfill Leachate

R. Kerry Rowe, F.ASCE[1]; and Yan Yu[2]

Abstract: A two-dimensional numerical model, BioClog, is used to estimate the leachate characteristics and leachate-induced clogging of laboratory mesocosms permeated with real municipal solid waste landfill leachate. The model is used to examine mesocosms with 38-mm (nominal diameter) gravel subjected to different durations of leachate permeation, mesocosms run-in series, and mesocosms with 19-mm gravel. A comparison of the calculated and measured leachate concentrations indicates that the model provided reasonable predictions of the effluent chemical oxygen demand (COD) and calcium concentrations. The calculated porosities within the saturated drainage layers are general in encouraging agreement with the measured values from all experimental mesocosms. The calculated and measured hydraulic conductivities are in reasonable agreement. The modeling results indicated that reducing the mass loading for the drainage layers and increasing the particle size of granular media can be expected to extend the time before clogging of drainage layers, and therefore, to extend the service life of landfill leachate collection systems. **DOI: 10.1061/(ASCE)GT.1943-5606.0000834.** © *2013 American Society of Civil Engineers.*

CE Database subject headings: Experimentation; Numerical models; Gravel; Landfills; Clogging.

Author keywords: Experimental cells; Numerical modeling; Leachate characteristics; Clogging; Leachate collection systems; Landfills.

Downloaded from ascelibrary.org by Queen's University Libraries on 06/19/14. Copyright ASCE. For personal use only; all rights reserved.

Introduction

Modern municipal solid waste (MSW) landfills are generally required to have a barrier system to minimize contaminant migration into the surrounding environment (Rowe et al. 2004; Rowe 2005). Two components are normally included in a barrier system: (1) a high permeability leachate collection system (LCS), and (2) an underlying low permeability liner. Although much has been written on liner performance (Bacas et al. 2011; Chappel et al. 2012; Eid 2011; Fox et al. 2011; Gudina and Brachman 2011; Rayhani et al. 2011; Rowe 2011, 2012a, b; Rowe et al. 2012), much less has been written on the other key component of the barrier system—the LCS. The LCS in a landfill is intended to allow the leachate within the granular drainage layer to freely drain to the perforated drainage pipes and from the pipes to sumps where the leachate is removed from the landfill for treatment. To reduce the potential impact on human health and the environment by the leakage of leachate into the groundwater and surface water, the leachate head on the bottom liner is typically required to be less than the design thickness of the granular drainage layer (0.3–0.5 m) (Rowe et al. 2004).

Field studies have shown that, when permeated with landfill leachate, the drainage material within the LCSs is prone to the development of a clog mass within the void spaces because of the biogeochemical processes that result in the growth of biomass, deposition of suspended particles, and precipitation of minerals [Bass 1986; Brune et al. 1991; Koerner et al. 1993, 1994; McBean et al. 1993; Rowe 1998; Fleming et al. 1999; Craven et al. 1999; Maliva et al. 2000; Bouchez et al. 2003; Levine et al. 2005 (EPA, Research Triangle Park, NC, unpublished internal report, 1982)]. The accumulation of clog mass, which reduces the porosity and hydraulic conductivity of drainage material, causes the leachate head to build up within the LCSs.

A numerical model, BioClog, was developed to model both laboratory column tests (Cooke et al. 2005a) and LCSs (Cooke and Rowe 2008a). Cooke et al. (2005b) and VanGulck and Rowe (2008) found that, for column experiments, the BioClog model gave a good estimate of the effluent leachate characteristics compared with the measured data. It also gave a good estimate of the clog mass within the porous media from the influent to the effluent end. Cooke and Rowe (2008b) used BioClog to model two laboratory mesocosms reported by McIsaac and Rowe (2007). The modeling results showed that the clog mass at the upper regions of the saturated gravel layer estimated by the numerical model agreed well with the measured values, whereas the model underestimated the clogging of gravel at lower regions. The BioClog model was enhanced by Yu and Rowe (2012a) to address this limitation of the original BioClog model.

The objective of this paper is to evaluate the performance of the enhanced BioClog model for predicting the changes in leachate characteristics and clogging of saturated gravel drainage layers by comparing the calculated performance with that observed in several laboratory mesocosms (Fleming 1999; Fleming and Rowe 2004; McIsaac 2007; McIsaac and Rowe 2007). Consideration will be given to the cells originally examined by Cooke and Rowe (2008b) with 38-mm gravel (C03, C04), mesocosms run-in series (C03-C23-C24-C25, C04-C26), and mesocosms with 19-mm gravel (C19, C20).

BioClog Model (Summary)

BioClog models the fate and transport of key constituents in leachate and the formation of clog mass within the porous media (Cooke and Rowe 2008a; Yu and Rowe 2012a). Three volatile fatty acids (acetate, butyrate, and propionate) are modeled because they contribute most

[1]Professor and Canada Research Chair in Geotechnical and Geoenvironmental Engineering, GeoEngineering Centre at Queen's-RMC, Dept. of Civil Engineering, Queen's Univ., Kingston, ON, Canada K7L 3N6 (corresponding author). E-mail: kerry@civil.queensu.ca

[2]Postdoctoral Fellow, GeoEngineering Centre at Queen's-RMC, Dept. of Civil Engineering, Queen's Univ., Kingston, ON, Canada K7L 3N6. E-mail: yan.yu@ce.queensu.ca

Note. This manuscript was submitted on December 21, 2011; approved on September 10, 2012; published online on September 12, 2012. Discussion period open until December 1, 2013; separate discussions must be submitted for individual papers. This paper is part of the ***Journal of Geotechnical and Geoenvironmental Engineering***, Vol. 139, No. 7, July 1, 2013. ©ASCE, ISSN 1090-0241/2013/7-1022–1034/$25.00.

of chemical oxygen demand (COD) in normal MSW leachate, and they are also relatively easily biodegraded, resulting, inter alia, in the production of carbonic acid, which is the source of carbonate that is a predominate contributor to clogging (Bennett et al. 2000; VanGulck et al. 2003). Both the suspended organic biomass and inorganic solids in leachate are modeled, where the suspended organic biomass includes the suspended active biomass and inert biomass, and the decay of the suspended active biomass is converted to the suspended inert biomass. The dissolved calcium in leachate is also modeled.

The clog mass within the porous media is quantified in terms of the thicknesses of five separate films attached to the surface of porous media (three active biofilms, inert biofilm, and inorganic solids film). The active biofilms (acetate, butyrate, and propionate degraders) increase the mass from the deposition of suspended active biomass and growth of active biofilms. They lose mass by decay and through detachment from the shear stress, as described in detail by Rittmann (1982). The inert biofilm increases the mass by the decay of active biofilms and from the deposition of suspended inert biomass. The inert biofilm decreases the mass through detachment from shearing. The inorganic solids film increases the mass from the deposition of suspended inorganic solid particles and precipitation of calcium carbonate and other minerals. In the enhanced BioClog model (Yu and Rowe 2012a), the deposition of suspended particles within the saturated porous media is modeled based on the attachment of suspended particles using a model proposed by Tien and Ramarao (2007), but is further modified to include a deposition factor where the effect of particle size range (0.001–0.1 mm) of sediment and microorganisms from real landfill leachate (Koerner and Koerner 1992; McIsaac 2007) was taken into account.

The finite-element method (FEM) is used to solve the partial differential equations for fluid flow and species transport (Istok 1989). The surface of the leachate mound is found using an iterative method (Cooke 2007). The increase in total thickness of films (the accumulation of clog mass) reduces the void spaces within the porous media. The porosity and specific surface of porous media are calculated with a geometric model (Yu and Rowe 2012b). The decrease in porosity causes a reduction in hydraulic conductivity of porous media that changes the flow field within the saturated drainage layer and results in leachate mounding into the previous unsaturated zone.

Laboratory Mesocosms

The laboratory mesocosms (Fig. 1) to be modeled were initiated by Fleming (1999) and have been described by Fleming and Rowe (2004) and McIsaac (2007). These mesocosms were designed to mimic the flow conditions near the drainage pipes in the landfill and to examine the clogging of LCSs subject to the permeation of real landfill leachate in real time and real scale (Fleming and Rowe 2004; McIsaac and Rowe 2006, 2007). This involved a great deal of patience because full-scale, real-time experiments take a considerable time to establish results. Each cell was 565-mm long, 235-mm wide, and 574-mm high. The base of each cell was filled by an approximately 40-mm-thick sand layer overlaid by a nonwoven geotextile with a slope of 1.5% to the effluent end. A 300-mm-thick layer of crushed dolomitic limestone gravel was placed over the geotextile. Above the gravel drainage layer was a layer of waste extracted from a landfill after biodegradation had commenced. The leachate from the Keele Valley landfill was introduced both above the waste (at a rate of 0.2 $m^3/m^2/a$) and from the horizontal port at the upgradient end of the mesocosm (with the average flow rate of 1.26 m^3/a, approximately simulating the same vertical infiltration rate over the 25-m drainage length to the perforated drainage pipe) (McIsaac and Rowe 2007). Leachate flowed through the saturated gravel layer into the perforations of drainage pipe and exited from the effluent port. A U-tube was attached to the effluent port to maintain a constant hydraulic head at the effluent end. All tests were operated under anaerobic conditions at 27 ± 2°C. Eight mesocosms (McIsaac and Rowe 2007) examining the effect of operation time, mass loading, and gravel size on the clogging of saturated gravel layer are modeled in this paper. The essential details for each mesocosm, as developed by Fleming and Rowe (2004), and whose maintenance over 12 years involved three generations of graduate students, are given in the following.

Mesocosms C03 and C04

Mesocosms C03 and C04 were essentially identical except for the time they were permeated with leachate. Both were filled with 38-mm gravel (D_{10} = 20 mm, D_{60} = 27 mm, D_{85} = 33 mm). The bottom 100 mm of the gravel drainage layer was initially saturated, and the

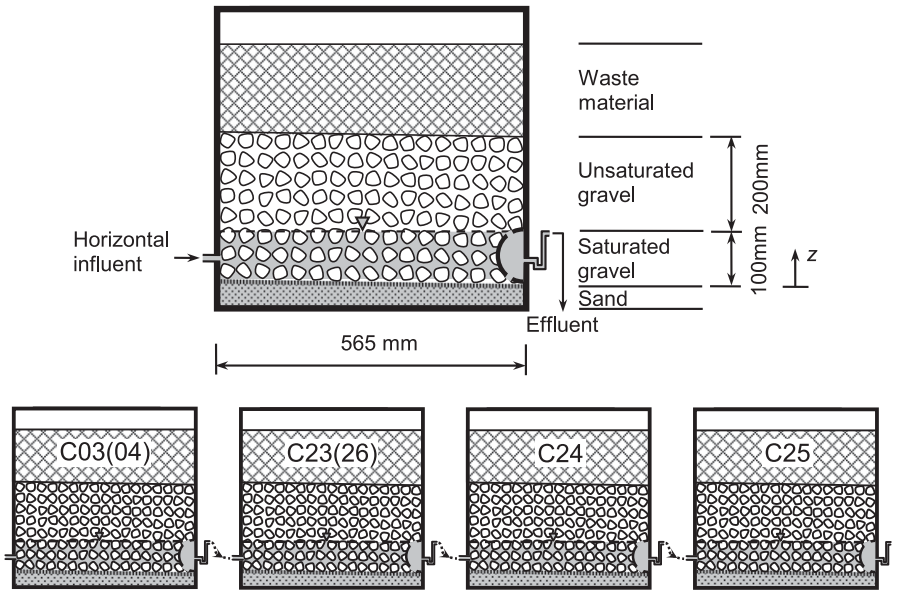

Fig. 1. Schematic showing the experimental mesocosm cells [data from McIsaac and Rowe (2007)]

J. Geotech. Geoenviron. Eng. 2013.139:1022-1034.

Downloaded from ascelibrary.org by Queen's University Libraries on 06/19/14. Copyright ASCE. For personal use only; all rights reserved.

rest of the drainage layer was unsaturated. Mesocosm C04 was exhumed after approximately 6 years, whereas mesocosm C03 was exhumed after 12 years. Mesocosms C03 and C04 were previously modeled by Cooke and Rowe (2008b) using the initial BioClog model (Cooke and Rowe 2008a). These mesocosms are re-examined in this paper using the enhanced BioClog model (Yu and Rowe 2012a).

Mesocosms Run-In Series C04-C26 and C03-C23-C24-C25

Because each mesocosm was 0.565-m long, these mesocosms were intended to examine clogging when leachate flows through a 1.13-m-long (C04-C26) and 2.26-m-long (C03-C23-C24-C25) gravel system by connecting the mesocosms in series, such that the leachate passing through the first mesocosm (C03 or C04) was input as the horizontal influent to the next mesocosm in the series (C23 or C26); for the second series, after flowing through this mesocosm, it became the influent to the next mesocosm (C24), whose outflow finally was the influent for the last mesocosm in the series (C25). All mesocosms received similar fresh [from Keele Valley Landfill (KVL)] leachate at a rate equivalent to approximately 0.2 m/year introduced above the waste overlying the gravel. Each of these mesocosms had a 300-mm thick layer of 38-mm gravel. Similar to mesocsoms C03 and C04 (described previously), the bottom 100 mm of gravel was saturated and the top 200 mm of gravel was unsaturated. After approximately 6 years of operation, mesocosms C23, C24, C25, C04, and C26 were exhumed to examine the clogging.

Mesocosms C19 and C20

Mesocosm C19 and its duplicate C20 both had a 300-mm-thick layer of 19-mm gravel ($D_{10} = 10$ mm, $D_{60} = 16$ mm, $D_{85} = 19$ mm). These mesocosms were similar to C03 and C04, except for the size of the gravel used. The bottom 100 mm of gravel drainage layer in each mesocosm was initially saturated, and the remaining 200-mm-thick gravel layer was initially unsaturated. These mesocosms (C19 and C20) were exhumed after approximately 6 years.

Modeling

Modeling involved two stages at each time step: (1) modeling of the flow region using the porosities and hydraulic conductivities established based on the transport modeling in the previous time step, and (2) transport modeling and assessment of the change in porosities and hydraulic conductivities because of clogging in this time step. The following subsections summarize the key aspects of the modeling and the relevant parameters.

Boundary Conditions for Modeling

The boundary conditions for the fluid flow involved a uniform infiltration rate of 0.2 m/year vertically into the saturated drainage layer on the top surface (Fig. 1). A line source on the influent end represented the leachate flux [Fig. 2(a)] from the horizontal influent port into the saturated drainage layer. In the numerical simulation, the location of this source was moved periodically for each mesocosm to correspond to changes in the location of the lateral source in each experiment (the location of the lateral source was changed periodically because of local clogging that occurred around the influent port) (McIsaac 2007). Details regarding the precise location of the inlet for a given mesocosm and time are given in Yu (2012). The remainder of the vertical boundary on the influent end and the bottom boundary were modeled as no flow boundaries. A constant specified head of 100 mm was applied over a zone from $z = 0$ to

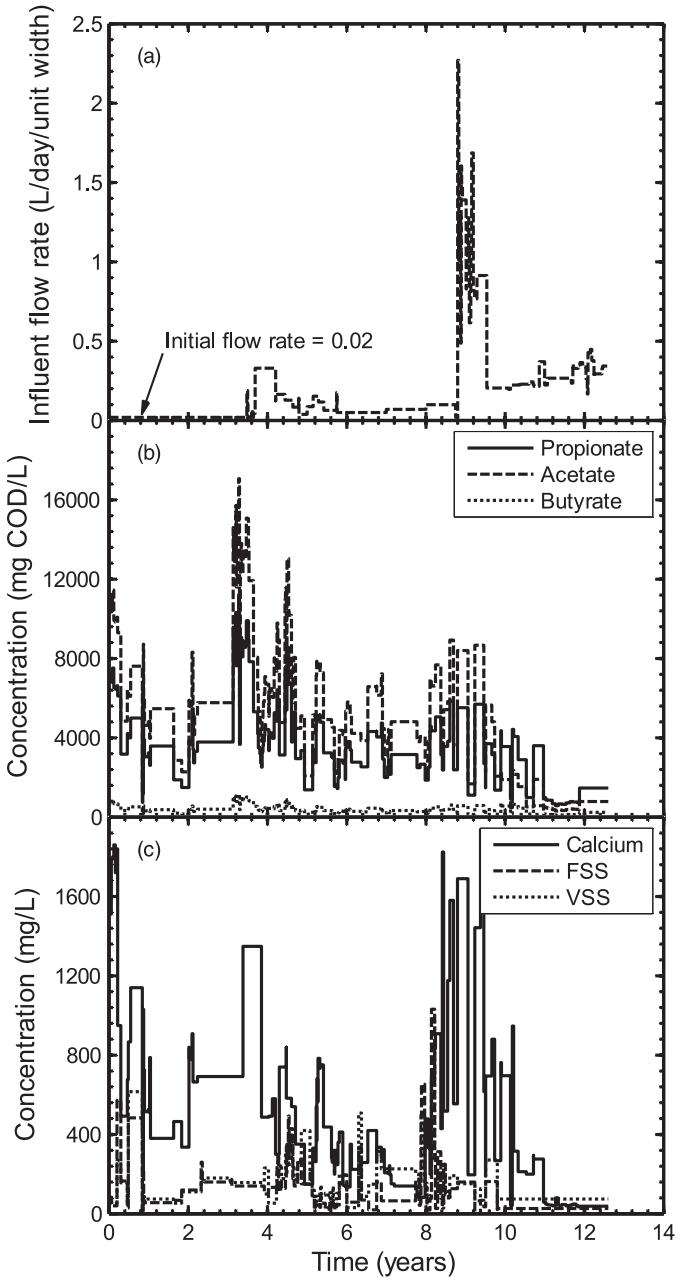

Fig. 2. Influent flow rates at the horizontal influent port and influent leachate concentrations: (a) influent flow rates; (b) volatile fatty acids concentrations; and (c) calcium, fixed suspended solids (FSS) volatile suspended solids (VSS) concentrations [Cooke and Rowe 2008b; Cooke, A. J., and Rowe, R. K. "Modelling landfill leachate induced clogging of field-scale test cells (mesocosms)," Canadian Geotechnical Journal, Vol. 45, Issue 11, 1497–1513, © 2008 Canadian Science Publishing or its licensors. Reproduced with permission]

$z = 30$ mm (where the lower perforations in the pipe were located) at the effluent end to correspond to the experiment conditions applied to the leachate level in the receptor pipe. The U-tube attached at the effluent port to keep the hydraulic head within the pipe to 100 mm (Fig. 1) was not explicitly modeled, although the effect was modeled. A no-flow boundary condition was applied to the remainder of the vertical boundary.

For species transport, the vertical infiltration of leachate was modeled as a Cauchy boundary (Padilla et al. 1997) with a time-varying

J. Geotech. Geoenviron. Eng. 2013.139:1022-1034.

Downloaded from ascelibrary.org by Queen's University Libraries on 06/19/14. Copyright ASCE. For personal use only; all rights reserved.

specific species total flux selected to correspond to the experimental data. The horizontal flow was modeled as a line source with a time-varying concentration based on experimental data. The effect of the waste and unsaturated gravel layer on the leachate characteristics from the vertical influent ports were not considered because the leachate causing the clogging of the saturated drainage layer was mostly from the lateral influent port in this experiment, and hence, the effect of the infiltration through the waste was minor in these particular experiments. The location of the line source varied somewhat depending on the mesocosm and time [because it had to be moved periodically because of clogging near the inlet as noted previously and as described by McIsaac (2007)]. The upstream vertical boundary (apart from the line source) and base were modeled as zero flux boundaries. The downstream vertical boundary was modeled as an open zone from $z = 0$ to $z = 30$ mm with a nonprescribed dispersive flux [the free-exit condition; Frind (1988)] to model the presence of the perforations in the drainage pipe at this location, and the remainder of this boundary was zero flux because of symmetry.

Finite-Element Model Mesh

The saturated gravel drainage layer in mesocosms C03 and C04 was modeled using 738 three-noded triangle elements and 420 nodes. A mesh with total 1,660 nodes and 2,952 three-noded triangle elements was used for modeling each of the four mesocosms in series C03(04), C23(26), C24, and C25. The mesh for modeling mesocosms C19 (20) was the same as that used for modeling mesocosms C03(04).

Porosity of Granular Material and Relationship between Hydraulic Conductivity and Porosity

The initial porosities of 38- and 19-mm gravel were 0.41 and 0.37, respectively (McIsaac 2007). The D_{60} value from the grading curve was used to represent the ideal grain size of granular material in the BioClog modeling. The D_{60} values were 27 and 16 mm for the 38- and 19-mm gravel, respectively. Based on experimental data (McIsaac 2007), the initial hydraulic conductivities were taken to be 0.12 and 0.03 m/s for the 38- and 19-mm gravel, respectively.

The accumulation of clog mass within the pore spaces decreases both the porosity and hydraulic conductivity of porous media when permeated with landfill leachate. An exponential relationship between the hydraulic conductivity and porosity was established for porous media based on laboratory data over a range of porosity (Armstrong 1998; Rowe et al. 2002; VanGulck 2003; VanGulck and Rowe 2004a, b; Cooke et al. 2005b)

$$k = A_k e^{b_k n} \tag{1}$$

where k = hydraulic conductivity of clogged porous media; n = porosity; and the coefficients A_k and b_k were obtained from the measured data with regression analysis. For the gravel modeled in this paper, the adopted values of A_k and b_k are given in Table 1 together with the applicable range in porosity.

Influent Flow Rates and Leachate Characteristics

The influent flow rates (Fig. 2) and leachate characteristics (Table 2 and Fig. 2) used as inputs for modeling mesocosms C03 (04) were based on Cooke and Rowe (2008b), Fleming (1999), and McIsaac (2007). The same influent flow rates and leachate characteristics for the first 6.2 years were used as input to the first mesocosm in the series C03-C23-C24-C25 and C04-C26, and to both mesocosms C19 and C20. These parameters were assumed to be constant between every two times when the flow rate and concentrations were measured. The same leachate was applied at both horizontal and vertical influent ports.

Table 1. Gravel Properties

Particle size	Hydraulic conductivity coefficient		
$d_g = D_{60}$ (mm)	A_k (m/s)	b_k	Applicable range in porosity (n)
27[a]	9.8×10^{-6}	22.9	$0.21 \le n \le 0.41$
	2.4×10^{-8}	51.0	$0 < n < 0.21$
16	3.5×10^{-7}	30.9	$0.21 \le n \le 0.37$
	2.0×10^{-8}	44.3	$0 < n < 0.21$

[a]Cooke and Rowe (2008b).

Table 2. Influent Leachate Characteristics [data from Cooke and Rowe (2008b)]

Parameters	Time period (years)	Value
f_{PAB}	0–9.7	0.905
f_{PAB}	9.7–12.6	0.6
VFA ratio (Pr:Ac:Bu)	0–9.7	0.38:0.58:0.04
VFA ratio (Pr:Ac:Bu)	9.7–12.6	0.59:0.32:0.09
VFAs, Ca, VSS, FSS (mg/L)	0–12.6	Variable (see Fig. 2)
VSS % active	0–12.6	70
VSS ratio Pr:Ac:Bu	0–12.6	1:1:1

Note: Ca = calcium; FSS = fixed suspended solids; f_{PAB} = fraction of chemical oxygen demand (COD) that is from propionate (Pr), acetate (Ac), and butyrate (Bu); VFA = volatile fatty acid; VSS = volatile suspended solids.

Fatty Acids and Biomass-Related Coefficients

The degradation rate for each fatty acid and the growth and decay of biomass are controlled by four kinetic rate coefficients (the maximum specific rate of substrate utilization, $\widehat{q}$; the half-maximum rate substrate concentration, K_s; the endogenous decay coefficient, b_d; and the maximum yield coefficient, Y). The values of these coefficients are influenced by many factors (Cooke and Rowe 2008b), and a large variation in values has been reported (Pavlostathis and Giraldo-Gomez 1991). Two sets of values for the kinetic rate coefficients (Case 1 and Case 2 listed in Table 3) were used by Cooke and Rowe (2008b) for modeling mesocosms C03(04). The Case 1 kinetic rate coefficients were values reported by Cooke et al. (2005b) using data from the laboratory columns operated at 21°C, and the Case 2 kinetic rate coefficients were values reported by Babcock (2005) and Rowe and Babcock (2007) using data from laboratory columns operated at 27°C. Both Cases 1 and 2 are considered in this paper.

The growth of each active biofilm (Rittmann and Brunner 1984) was evaluated from the flux of substrate into the biofilm through the effective diffusion layer (Rittmann and McCarty 1981). The coefficients of molecular diffusion of substrates in the free solution, D_o and within the biofilm D_f (Table 3), were based on measured values reported by Yu and Pinder (1994) at 35°C. The thickness of the effective diffusion layer was calculated by a method proposed by Yu and Rowe (2012a) that was modified from Wilson and Geankoplis (1966). The fraction of active biomass degradable by decay was taken to be 0.8 (Rittmann and Snoeyink 1984). The mass from decay of active biomass that was not degraded was converted to the inert biomass.

Clog Mass Parameters

Provided that there was sufficient calcium available in the leachate to precipitate, the amount of clog mass from the precipitation of calcium carbonate was based primarily on the production of carbonic acid generated by the biodegradation of the volatile fatty acids in the

J. Geotech. Geoenviron. Eng. 2013.139:1022-1034.

Downloaded from ascelibrary.org by Queen's University Libraries on 06/19/14. Copyright ASCE. For personal use only; all rights reserved.

Table 3. Fatty Acid and Biomass Related Parameters [data from Cooke and Rowe 2008b)

Parameters	Propionate	Acetate	Butyrate
Kinetic constants			
K_s (case 1) (mg COD/L)	4700	4700	4060
$\widehat{q}_{Max}$ (case 1) (mg COD/mg VS/d)	1.0	1.76	5.2
K_s (case 2) (mg COD/L)	1600	1790	1230
$\widehat{q}_{Max}$ (case 2) (mg COD/mg VS/d)	2.0	3.0	2.0
A_q	80	80	80
B_q	4	4	4
Y (mg VS/mg COD)	0.02	0.04	0.025
b_d (d^{-1})	0.02	0.018	0.02
Diffusion parameters			
D_0 (substrate in fluid) (cm^2/d)	1.27	1.50	1.11
D_f (substrate in film) (cm^2/d)	0.52	0.47	0.31

Note: A_q and B_q = parameters for the dynamic specific rate of substrate utilization; b_d = endogenous decay rate; D_0 and D_f = coefficients of molecular diffusion in the free solution and within the biofilm, respectively; K_s = half-maximum rate substrate concentration; $\widehat{q}_{Max}$ = maximum value of the specific rate of substrate utilization; VS = volatile solids; Y = maximum yield coefficient.

leachate multiplied by the carbonic acid yield coefficient (VanGulck et al. 2003). The maximum value of carbonic acid yield coefficient $Y_{H,Max}$ was set to 0.05 based on experimental data (Cooke et al. 2005b). The availability of calcium was modeled, and as the calcium concentration approached zero, the precipitation was reduced to zero as described in Yu (2012). The ratio of the volume of mineral precipitation (other than calcium carbonate) to the volume of calcium carbonate precipitated [f_{OP}; Cooke et al. (2005a)] was set to 0.06 as measured in column experiments by VanGulck and Rowe (2004b). Based on experimental data from McIsaac (2007), the formation of clog mass in the unsaturated zone just above the surface of the leachate mound was modeled as described by Yu and Rowe (2012a) using parameters given in Table 4 ($A_{Lf} = 0.0025$ and $B_{Lf} = 4.4$). The density of biofilm was evaluated using parameters (A_X and B_X) given in Table 4, which are based on experimental data (Cooke et al. 2005a). The inorganic film density was taken to be 2,750 mg/cm^3 as measured by VanGulck et al. (2003).

Suspended Particles–Related Parameters

The deposition of suspended particles on the surface of porous media was modeled based on Tien and Ramarao (2007) and a deposition factor as described in Yu and Rowe (2012a). The organic and inorganic particle densities (Table 4) were based on VanGulck (2003) and VanGulck and Rowe (2008). The effective diameter for the organic particles was taken to be 0.0001 cm (Metcalf and Eddy, Inc. 1991). The inorganic particles had an effective diameter of 0.0002 cm, which was within the range of particle sizes found in landfill leachate (Koerner and Koerner 1992). The deposition factor parameters A_{SP} and B_{SP} were taken to be 40 and 5, respectively (Table 4). The shear stress (Rittmann 1982) was considered for modeling the detachment of biofilms. It was assumed that there was no detachment for inorganic film. The inert biofilm detachment was limited by the protection coefficient $P = 0.00104$ cm (Cooke et al. 2005a; Cooke and Rowe 2008b).

Other Parameters

The same time step was used for modeling the fluid flow and for modeling the species transport. The time step was 0.025 day from 0 to 3.5 years, 0.01 day from 3.5 to 8.6 years, and 0.0025 day from 8.6 to 12.6 years for mesocosms C03(04), C23(26), C24, and C25.

Table 4. Parameters for Suspended Particles and Formation of Clog Mass

Parameters	Value
Clog matter parameters	
Maximum carbonic acid yield coefficient, $Y_{H,Max}$	0.05[a]
Carbonic acid yield coefficient parameter, A_{YH}	80
Carbonic acid yield coefficient parameter, B_{YH}	4
Film thickness parameter for unsaturated zone, A_{Lf}	0.0025
Film thickness parameter for unsaturated zone, B_{Lf}	4.4
Initial film thickness coefficient, f_{Init}	0.8
Variable biofilm density parameter, A_X	247[b]
Variable biofilm density parameter, B_X (mg VS/cm^3)	72[b]
Inorganic film density, $X_{f,IS}$ (mg NVS/cm^3)	2,750[c]
Precipitate ratio, f_{OP}	0.06[d]
Fraction degradable by decay, f_d	0.8[e]
Suspended solids parameters	
Active and inert diameter (cm)	0.0001[f]
Active and inert density (mg VS/cm^3)	1,030[g]
Inorganic particles diameter (cm)	0.0002[h]
Inorganic particles density (mg NVS/cm^3)	1,065[g]
Filter-separator coefficient, $f_{FS,SD}$	1.0
Filter-separator coefficient, $f_{FS,IB}$	1.0
Filter-separator coefficient, $f_{FS,IB}$	1.0
Deposition factor parameter, A_{SP}	40
Deposition factor parameter, B_{SP}	5
Attachment and detachment	
Single spherical collector efficiency, η_g	Tien and Ramarao (2007)
Collision efficiency for spherical collector, ψ_g	0.8
Shear detachment modifier	1.0[i]
Protection parameter, P (cm)	0.00104[b]
Growth detachment modifier	1.0[i]

Note: VS, volatile solids; $X_{f,IS}$, mass of nonvolatile solids (NVS) per volume of inorganic solids.
[a]Cooke et al. (2005b).
[b]Cooke et al. (2005a).
[c]VanGulck et al. (2003).
[d]VanGulck and Rowe (2004b).
[e]Rittmann and Snoeyink (1984).
[f]Metcalf and Eddy, Inc. (1991).
[g]VanGulck and Rowe (2008).
[h]Koerner and Koerner (1992).
[i]Cooke and Rowe (2008a).

The time step was 0.0025 day for mesocosms C19(20). The longitudinal dispersivity of saturated gravel was increased as the porosity reduced because of the clogging of porous media (Table 5) based on an equation (Cooke and Rowe 2008a) modified from Taylor and Jaffe (1990). The transverse dispersivity was assumed to be the same as the longitudinal dispersivity because of the relatively uniform nature of the media and small scale modeled.

Results and Discussion

Effluent Chemical Oxygen Demand

The measured and calculated effluent CODs for mesocosms C03 (from 0 to 12.6 years) and C04 (from 0 to 6 years) with 38-mm gravel are shown in Fig. 3. Over the first 6 years, mesocosms C03 and C04 were nominally identical, and hence, the variation in experimental data shown in Fig. 3 indicates the experimental variability that can occur in these systems. The effluent CODs calculated for Case 1 were higher than those for Case 2 because of the lower microbial activity

J. Geotech. Geoenviron. Eng. 2013.139:1022-1034.

Downloaded from ascelibrary.org by Queen's University Libraries on 06/19/14. Copyright ASCE. For personal use only; all rights reserved.

Table 5. Two-Dimensional Numerical Parameters and Relationship between Dispersivity and Porosity for Gravel (from Cooke and Rowe 2008b)

Parameters	Value
Numerical settings	
Time step, Δt (d)	Variable (see text)
Relaxation factor, ω	1.0
Substrate convergence tolerance, ε	0.001
Surface convergence tolerance, ε_{HZ}, ε_{ZZ}	0.05
Surface extrapolation multiplier, E_f	1.0
Limit surface node movement	No
Element orientation	All right oriented
Limits	
Minimum hydraulic conductivity, k_{Min} (m/s)	1×10^{-8}
Minimum saturated thickness, γ_{Min} (cm)	0.3
Dispersivity	
Longitudinal dispersivity, α_L (cm)	$\alpha_L = \alpha_{L,0}\left(\frac{n}{n_0}\right)^{b_\alpha}$
Initial longitudinal dispersivity, $\alpha_{L,0}$ (cm)	1.0
Equation parameter, b_a	−1.74
Transverse dispersivity, α_T(cm)	$\alpha_T = c_\alpha \alpha_L$
Equation parameter, c_α	1.0

associated with the Case 1 parameters, resulting in the lower utilization of fatty acids. For the first 0.2 years, there was limited reduction in effluent COD (compared with the influent values), because during this period the biofilm was becoming established on the saturated gravel. After 0.2 years, the ratio of effluent to influent COD started to decrease because of the consumption of fatty acids by the established biofilm, and at approximately 1 year, the normalized COD was below 0.4 for Case 1 and below 0.2 for Case 2. Between 3.1 and 3.5 years, influent fatty acid concentrations (and hence, COD) were greatly elevated [Fig. 2(b)], which resulted in correspondingly relatively high calculated effluent CODs. However, there was still a significant reduction in concentration, with a ratio of effluent to influent COD between 0.2 and 0.8 for Case 1 and between 0 and 0.4 for Case 2 during this period as a result of leachate treatment within the mesocosms. When the leachate flow rate increased at approximately 8.8 years [Fig. 2(a)], there was an increase in the calculated effluent CODs [Fig. 3(b)] because of the shorter residency time for the leachate in the mesocosm, resulting in less consumption of fatty acids, and hence, COD. All measured CODs from the effluent of mesocosm C04 were bracketed by the calculated values for Cases 1 and 2. This was also generally true for mesocosm C03, but with exceptions at approximately 2.1 years, three points between 5 and 6 years, and one point at approximately 8.1 years. However, given a set of parameters based on column tests (Cases 1 and 2), the effluent CODs calculated using BioClog were in encouraging agreement with the observed values, and the kinetic rate coefficients for Cases 1 and 2 generally bracketed the scatter of the observed behavior.

Fig. 4 shows the measured and calculated effluent CODs for mesocosms C23(26), C24, and C25. The leachate from the effluent of mesocosms C03(04) was the source leachate for mesocosms C23 (26). Except for a few stray experimental data points (that were not consistent between the two duplicate mesocosms C23 and C26), the calculated effluent CODs from these mesocosms for Cases 1 and 2 were generally bracketing the observed values [Fig. 4(a)] and in encouraging agreement, allowing for the variability of biological systems. A similar conclusion can be reached for the third [C24; Fig. 4(b)] and fourth [C25; Fig. 4(c)] mesocosms in the series.

The measured effluent CODs for duplicate mesocosms C19 and C20 with nominal 19-mm gravel (Fig. 5) were generally consistent, with a few data points for the two mesocosms differing significantly at a few times, again highlighting the variability of biological systems as previously noted for the mesocosms with 38-mm gravel. The

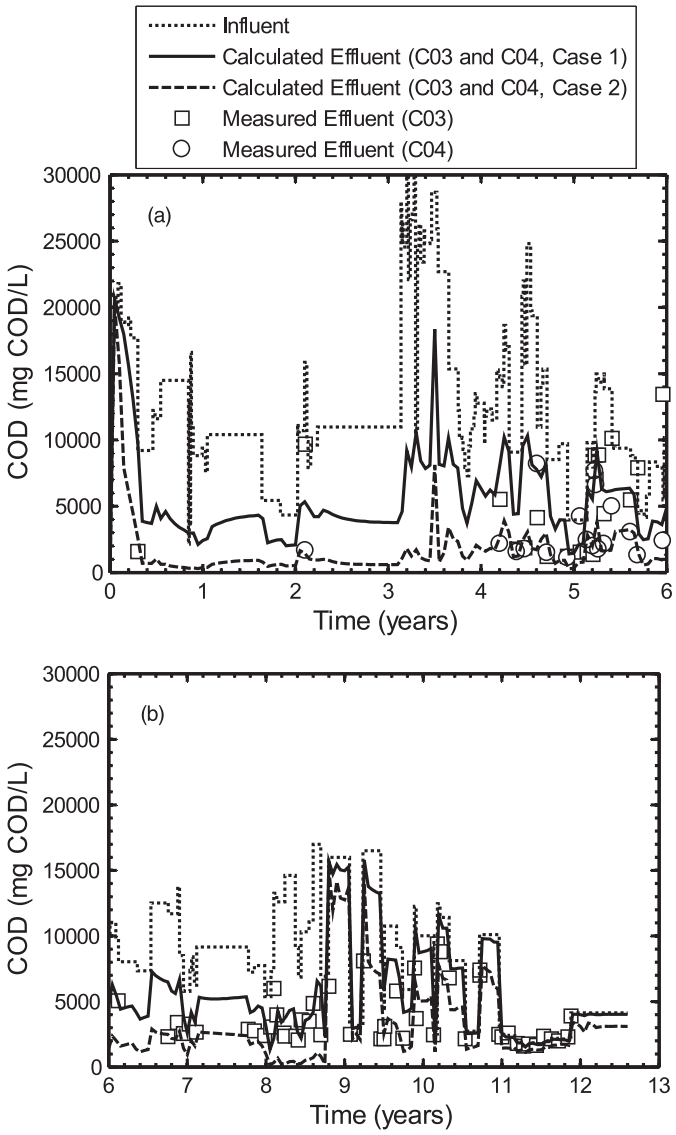

Fig. 3. Effluent CODs for mesocosms C03(04) filled by the 38-mm gravel: (a) 0–6 years; and (b) 6–12.6 years [measured COD values from Fleming (1999) and McIsaac (2007)]

calculated effluent CODs for Cases 1 and 2 again generally provided a good bracketing of the measured effluent COD values.

Effluent Calcium

The calculated and measured effluent calcium concentrations for mesocosms C03 and C04 (38-mm gravel) are shown in Fig. 6 up to 12.6 years. The depletion of calcium concentration from leachate calculated by the model was associated with the production rate of carbonic acid and a carbonic acid yield coefficient (VanGulck et al. 2003). The calculated effluent calcium concentrations obtained for Case 2 were lower than those for Case 1 because the greater microbial activity associated with Case 2 parameters resulted in greater generation of carbonic acid in leachate, and hence, greater precipitation of calcium carbonate. The calculated effluent calcium concentrations for Case 2 were generally closer to the measured values than those from Case 1; however, in general, the model gave the calculated calcium concentrations encouraging general agreement with the observed values.

J. Geotech. Geoenviron. Eng. 2013.139:1022-1034.

Downloaded from ascelibrary.org by Queen's University Libraries on 06/19/14. Copyright ASCE. For personal use only; all rights reserved.

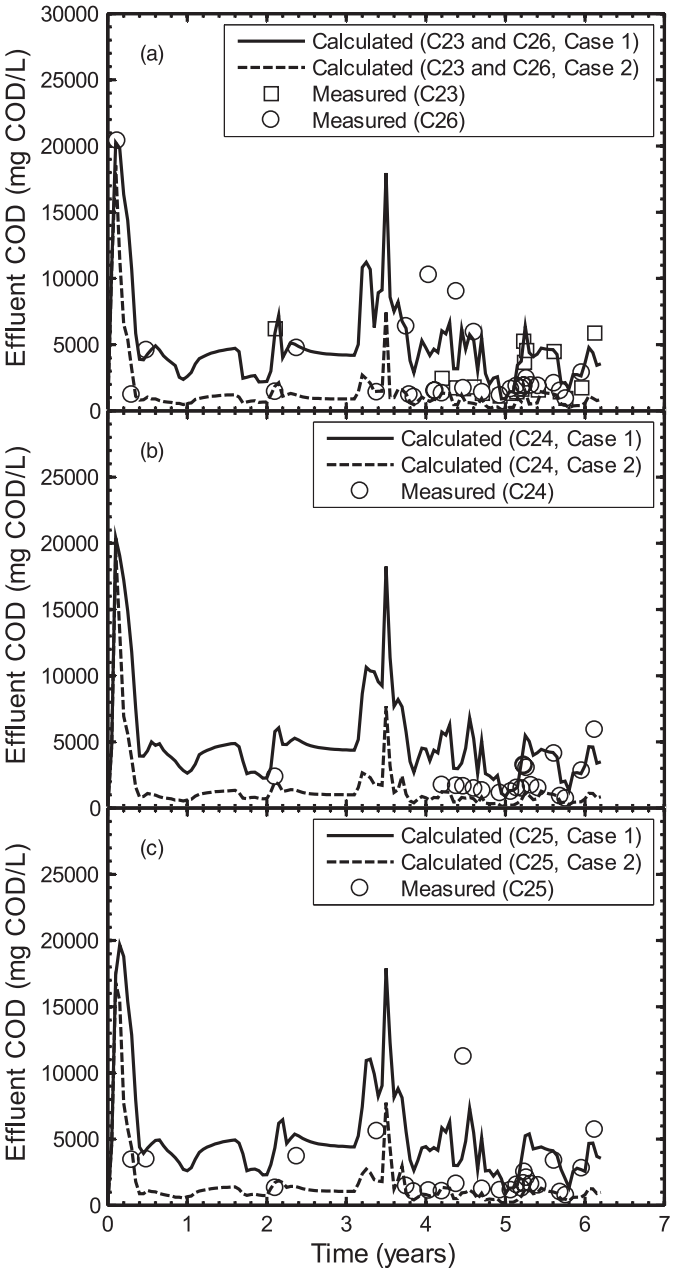

Fig. 4. Effluent CODs for mesocosms C23(26)-C24-C25 run-in series filled by the 38-mm gravel: (a) C23(26); (b) C24; and (c) C25 [measured COD values from Fleming (1999) and McIsaac (2007)]

As was the case for mesocosms C03 and C04, for the mesocosms in the series behind these mesocosms [C23(26), C24, and C25; Fig. 7], the predictions for Case 2 kinetic parameters were closer to the observed values. Generally, the model captures the effluent concentrations from the various mesocosms reasonably well, but with a tendency to overestimate the calcium concentration (and hence, the clogging). However, it should be remembered that these are genuine predictions with the kinetic parameters being based on independent column tests (they were not adjusted to fit the experimental data from the mesocosms). Better fits could have been obtained by calibrating the parameters to fit the data.

The calculated and measured effluent calcium concentrations for mesocosms C19(20) with 19-mm gravel (Fig. 8) followed similar trends to those noted previously for the 38-mm gravel, with the calculated effluent calcium concentrations from Case 2 being closer

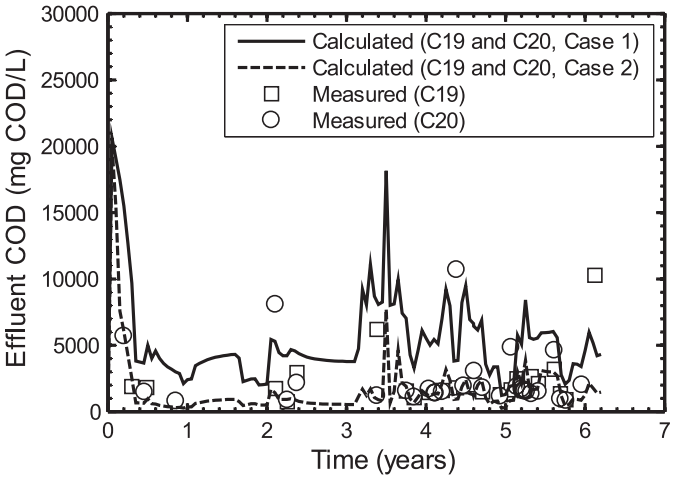

Fig. 5. Effluent CODs for mesocosms C19(20) filled by the 19-mm gravel [measured COD values from Fleming (1999) and McIsaac (2007)]

to the measured data than for Case 1, with the calculated concentrations slightly overestimating the measured values.

Porosity of Clogged Gravel

The average observed porosities within the saturated zone for mesocosms C03 and C04 (38-mm gravel) after exhumation of the mesocosms at 6 [Fig. 9(a)] and 12.6 years [Fig. 9(b)], respectively, are presented for six zones (an influent zone, middle zone, and effluent zone with the upper and lower region for each zone). Comparison of the observed porosities with the calculated porosities shown in Figs 9(a and b) indicates that in both cases the porosity was (1) lower in the bottom half of the saturated zone than in the upper half at both times, (2) lowest near the influent end (where the highest leachate strength was present) at both times and near the perforations in the pipe at the effluent end (where the flow, and hence, mass loading was greatest) after 12.6 years, and (3) lower (implying more clogging) after 12.6 years than after 6 years. Fig. 9(b) also showed that because of clogging of the lower gravel layer, after 12.6 years, the leachate had risen into the previous unsaturated zone, which resulted in a relatively high porosity zone near the surface.

For mesocosms C03(04) at 6 years [Fig. 9(a)], the clogging of gravel at the influent zone was slightly overestimated by the model, with the calculated average porosities of 0.13 and 0.05 at the upper and lower regions, respectively, compared with measured average porosities of 0.18 at the upper region and 0.12 at the lower region. In the middle zone, the average porosity of gravel was well calculated in the upper region by the model, with a measured value of 0.25 compared with a calculated one of 0.24, whereas it was slightly underestimated in the lower region, where the measured and calculated values were 0.09 and 0.15, respectively. In the effluent zone, the measured average porosity of 0.30 in the upper region agreed well with the calculated average porosity of 0.31, whereas the model slightly overestimated the average porosity measured (0.12) in the lower region (the calculated value was 0.19).

For mesocosms C03(04) at 12.6 years [Fig. 9(b)], the measured and calculated average porosities, which were generally in good agreement in the upper regions of the saturated drainage layer from the influent, middle, and effluent zones, were 0.11 and 0.13, 0.17 and 0.18, and 0.20 and 0.22, respectively. The clogging of gravel in the lower region of the influent zone was so severe that the measured average porosity was close to zero compared with the calculated

J. Geotech. Geoenviron. Eng. 2013.139:1022-1034.

Downloaded from ascelibrary.org by Queen's University Libraries on 06/19/14. Copyright ASCE. For personal use only; all rights reserved.

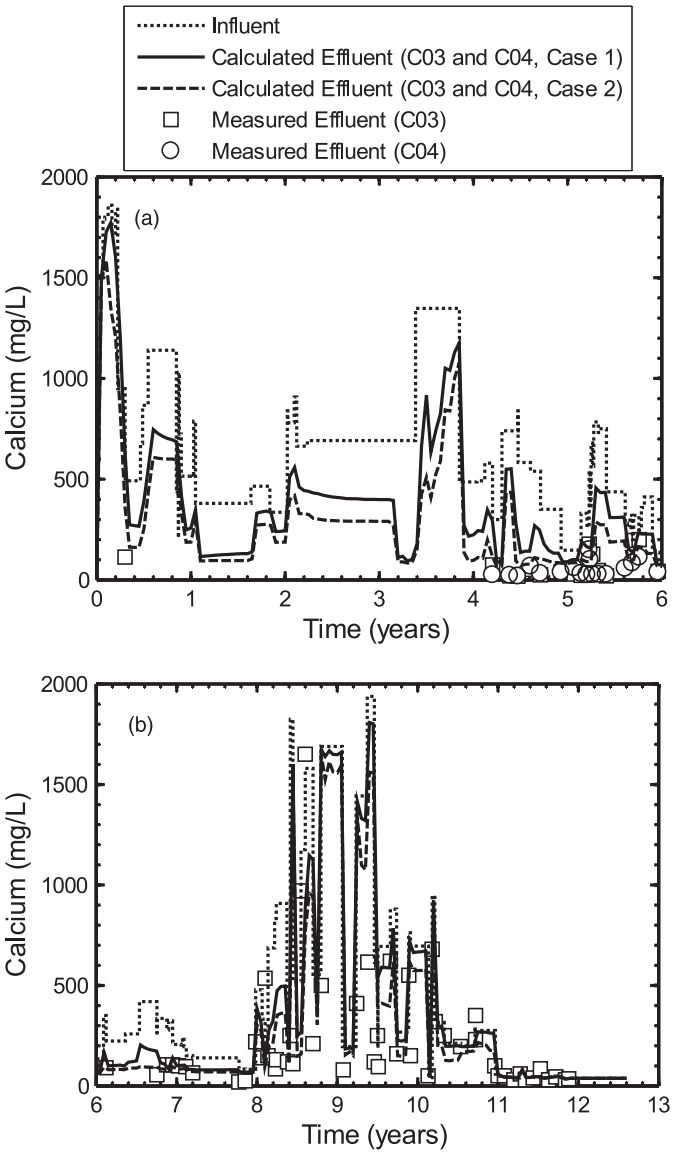

Fig. 6. Effluent calcium concentrations for mesocosms C03(04) filled by the 38-mm gravel: (a) 0–6 years; and (b) 6–12.6 years [measured Ca values from Fleming (1999) and McIsaac (2007)]

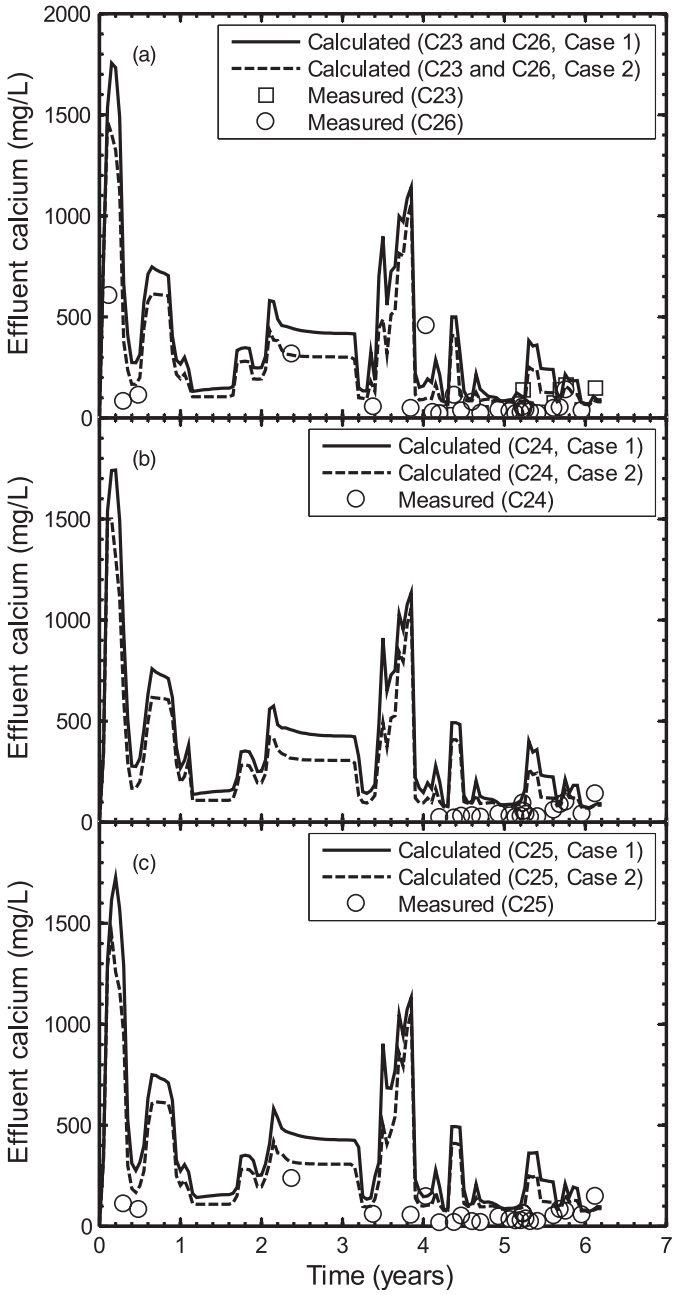

Fig. 7. Effluent calcium concentrations for mesocosms C23(26)-C24-C25 run-in series filled by the 38-mm gravel: (a) C23(26); (b) C24; and (c) C25 [measured Ca values from Fleming (1999) and McIsaac (2007)]

average value of 0.04 [Fig. 9(b)]. In the lower region of the middle zone, the measured and calculated average porosities were in good agreement (0.09 versus 0.11). In the lower region of the effluent zone, the calculated average porosity of 0.11 was higher than the measured 0.02 indicated, which the model underestimated in the clogging of gravel in this region.

Fig. 10 shows the porosity of 38-mm gravel within the saturated drainage layer at 6.2 years for the mesocosms C23(26), C24, C25 run-in series. The results from both the measured and calculated porosities showed that the clogging of gravel within the saturated drainage layer from the first to the last mesocosm in the series was reduced because of the reduced leachate strength along the flow path. For mesocosms C23(26), as shown in Fig. 10(a), the measured average porosities of 0.35, 0.36, and 0.36 at the upper regions from the influent, middle, and effluent zones, respectively, were estimated well by the model, where the calculated average porosities from the influent, middle, and effluent zones were 0.34, 0.36, and 0.38, respectively. The calculated average porosity (0.23) in the lower region of the influent zone slightly overestimated the measured value (0.19). In the lower region of the middle zone, the calculated average porosity (0.28) agreed well with the measured value (0.26). In the lower region of the effluent zone, the clogging of gravel was slightly underestimated, with a calculated average porosity of 0.33 compared with the measured 0.27. For the third mesocosm in the series [C24; Fig. 10(b)], the clogging of gravel was estimated well by the model, with the greatest discrepancy being in the lower region of the effluent zone where the measured average porosity was 0.33 compared with a calculated value of 0.36. For the last mesocosm in the series [C25; Fig. 10(c)], the model provided good predications of the porosities in all six regions.

Fig. 11 shows the measured and calculated porosities of 19-mm gravel in mesocosms C19(20). The measured average porosity of

J. Geotech. Geoenviron. Eng. 2013.139:1022-1034.

Downloaded from ascelibrary.org by Queen's University Libraries on 06/19/14. Copyright ASCE. For personal use only; all rights reserved.

0.12 in the upper region of the influent zone was generally estimated well by the model with a calculated value of 0.10. In the lower region of the middle zone, the clogging of gravel was slightly overestimated, where the calculated average porosity was 0.12 compared with the measured 0.15. In the effluent zone, the model generally estimated well the clogging of gravel in the upper region (with the measured average porosity of 0.23 compared with the calculated value of 0.25), whereas it slightly underestimated the measured average porosity of 0.19 in the lower region (the calculated value was 0.16).

Hydraulic Conductivity of Clogged Gravel

The calculated hydraulic conductivities within the saturated drainage layer for mesocosms C03 and C04 with 38-mm gravel at 6 [Fig. 12(a)] and 12.6 years [Fig. 12(b)] generally increased from the influent to effluent end because of the reduction in clog mass accumulating within the drainage material along the flow path, except where the flow, and therefore, mass loading was concentrated near the open zone at the effluent boundary (from $z = 0$ to 0.03 m). After 6 years, the calculated minimum hydraulic conductivity of gravel in the lower region of the influent zone [Fig. 12(a)] had dropped to less than 1×10^{-7} m/s, a six-order magnitude reduction from the initial value of 0.12 m/s. In the lower region of the effluent zone, the hydraulic conductivity of gravel near the effluent open zone was less than 1×10^{-4} m/s, a reduction by three orders of magnitude. After 12.6 years [Fig. 12(b)], the reduction in the drainage ability of gravel had caused leachate to build up into the previous unsaturated zone, and the hydraulic conductivity of gravel near the effluent open zone was reduced by five orders of magnitude to less than 1×10^{-6} m/s. The measured hydraulic conductivities over the full saturated thickness at 0.1-m intervals (the first five sections with a length of 0.1 m and the last section with a length of 0.065 m) (McIsaac 2007) of 2×10^{-5} to 8×10^{-5} m/s (section 1), 4×10^{-5} to 2×10^{-4} m/s (section 2), 9×10^{-5} to 3×10^{-4} m/s (section 3), 3×10^{-4} to 4×10^{-3} m/s (section 4), 1×10^{-4} to 9×10^{-4} m/s (section 5), and 1×10^{-4} to 4×10^{-4} m/s (section 6) were reasonably consistent with the calculated geometric means of 3×10^{-6}, 2×10^{-5}, 7×10^{-5}, 1×10^{-4}, 2×10^{-4}, and 9×10^{-5} m/s from the first section to the last section along the flow path [Fig. 12(b)]. Fig. 12 also shows that the difference in the hydraulic conductivity of gravel within the saturated drainage layer was more than five orders of magnitude, with the lowest hydraulic conductivity in the lower region of the influent zone caused by the highest mass loading received in this region and the highest hydraulic conductivity in the upper region of effluent zone caused by the lowest mass loading.

For mesocosms C19(20) with 19-mm gravel (Fig. 13), the calculated minimum hydraulic conductivity of gravel was reduced by more than 5 orders of magnitude from the initial value of 0.03 m/s to less than 1×10^{-7} m/s in the lower region of the influent zone. Near the effluent open zone, the reduction in hydraulic conductivity was more than four orders of magnitude, and the hydraulic conductivity had dropped to less than 1×10^{-6} m/s at 6.2 years. The modeling

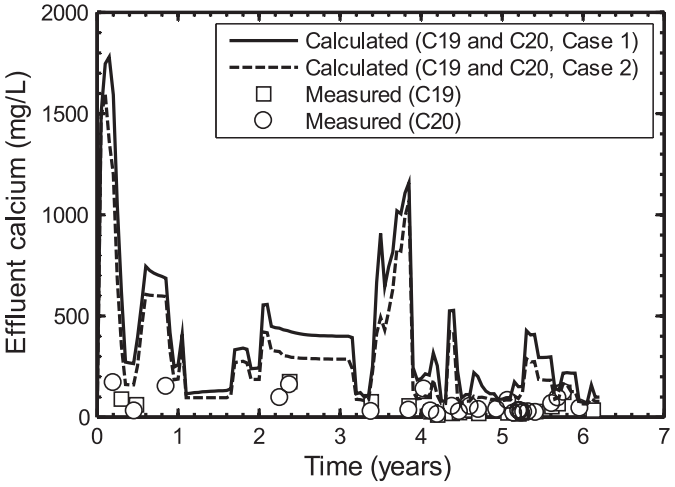

Fig. 8. Effluent calcium concentrations for mesocosms C19(20) filled by the 19-mm gravel [measured Ca values from Fleming (1999) and McIsaac (2007)]

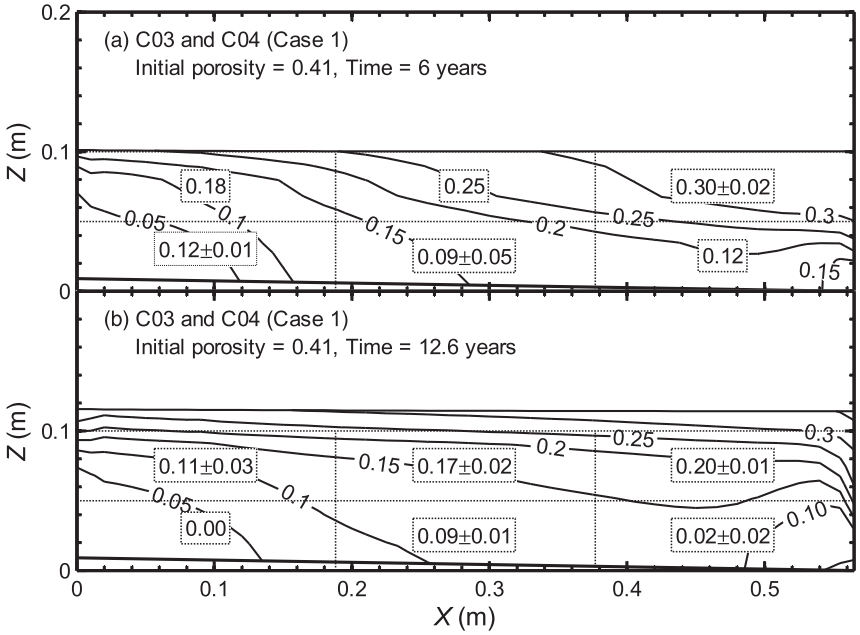

Fig. 9. Calculated porosities within the saturated drainage layer for mesocosms C03(04) with 38-mm gravel at (a) 6 years; (b) 12.6 years [measured values shown in boxes from McIsaac (2007)]

J. Geotech. Geoenviron. Eng. 2013.139:1022-1034.

Downloaded from ascelibrary.org by Queen's University Libraries on 06/19/14. Copyright ASCE. For personal use only; all rights reserved.

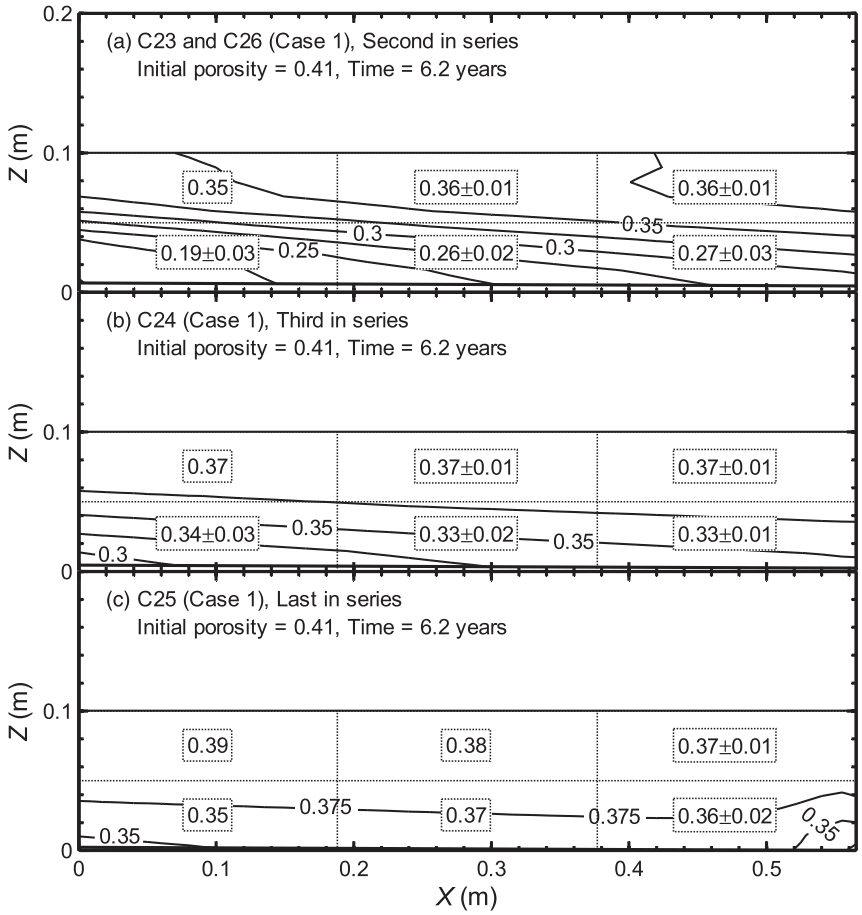

Fig. 10. Calculated porosities within the saturated drainage layer for mesocosms with 38-mm gravel run in series at 6.2 years (a) mesocosms C23(26); (b) mesocosm C24; (c) mesocosm C25 [measured values shown in boxes from McIsaac (2007)]

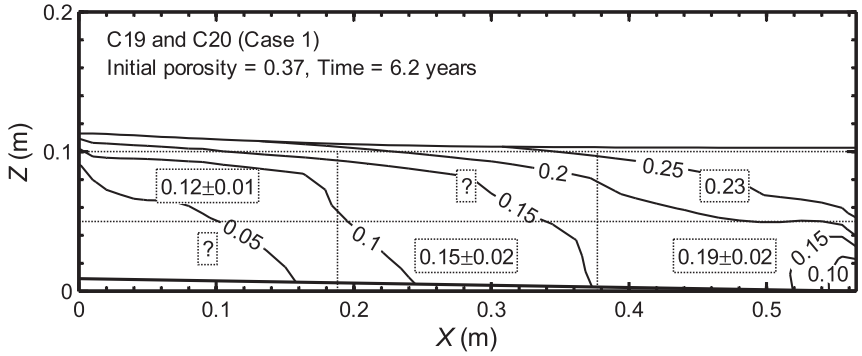

Fig. 11. Calculated porosities within the saturated drainage layer for mesocosms C19(20) with 19-mm gravel at 6.2 years [measured values shown in boxes from McIsaac (2007)]

results also showed that the difference in hydraulic conductivity of 19-mm gravel within the saturated drainage layer was more than four orders of magnitude, and the clogging of 19-mm gravel caused the leachate to mound into the previous unsaturated zone within 6.2 years. McIsaac and Rowe (2007) reported that near the influent end, the measured average hydraulic conductivity of 19-mm gravel was approximately 2.7×10^{-5} m/s through the first 0.12-m section after 6 years, which was lower than that of 38-mm gravel (5.2×10^{-5} m/s through the first 0.1-m section) after approximately 12.6 years. The modeling results showed that after a similar time period of leachate permeation, the calculated hydraulic conductivities of 19-mm gravel (Fig. 13) were lower than those of 38-mm gravel [Fig. 12(a)], therefore causing a lower drainage capacity of 19-mm gravel than 38-mm gravel.

Practical Implications

The model correctly predicted the change in clogging of the 38-mm gravel after both 6 and 12 years of permeation of landfill leachate and

J. Geotech. Geoenviron. Eng. 2013.139:1022-1034.

Downloaded from ascelibrary.org by Queen's University Libraries on 06/19/14. Copyright ASCE. For personal use only; all rights reserved.

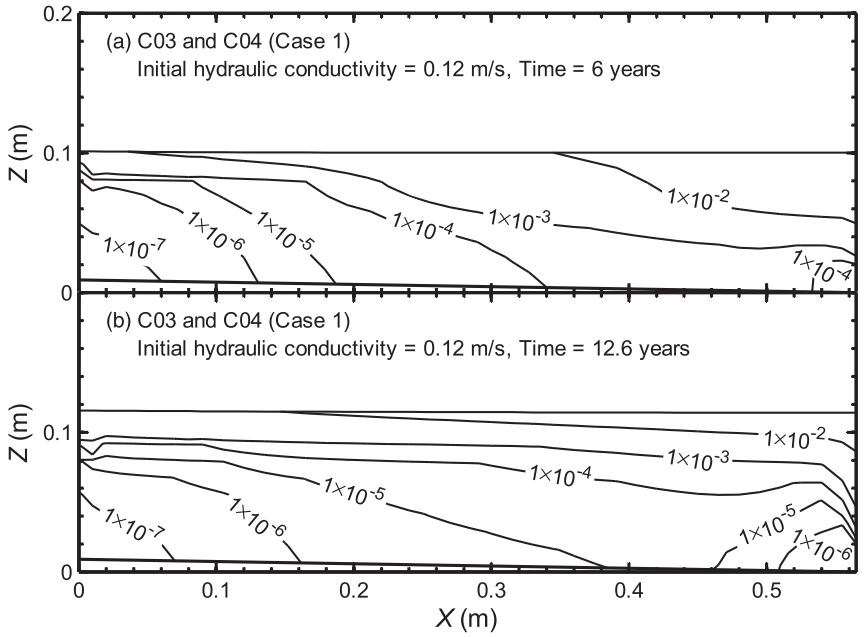

Fig. 12. Calculated hydraulic conductivities within the saturated drainage layer for mesocosms C03(04) with 38-mm gravel at (a) 6 years; (b) 12.6 years

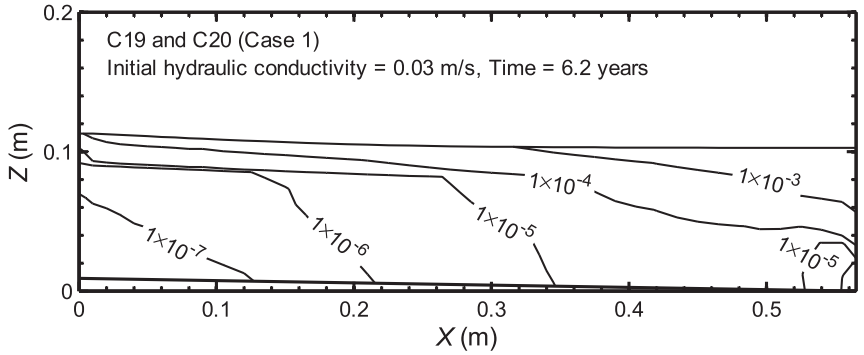

Fig. 13. Calculated hydraulic conductivities within the saturated drainage layer for mesocosms C19(20) with 19-mm gravel at 6.2 years

also correctly predicted the increase in the leachate level into the previous unsaturated zone at approximately 12 years because of clogging of the lower saturated drainage material. It confirmed that clogging is greatest where the mass loading is greatest (in this case near the influent port and near the perforations of the leachate collection pipe). These results show that clogging of even coarse (38-mm) gravel can be expected in a LCS, but by maintaining a relatively low saturated leachate level, the clogging of a coarse gravel layer by normal MSW leachate will take a long time. In this case, after 12 years, the leachate level had only risen approximately 1.4 cm and with approximately 18.6 cm of high permeability gravel remaining to be clogged before the leachate level had reached a height of 30 cm (i.e., to the top of the gravel layer). However, it is also evident from these results that the leachate level would ultimately have been controlled by the clogging near the perforations in the pipe.

The model also correctly predicted the effect of particle size and confirmed empirical experience that for a relatively uniform granular media, the coarser the particle size, the slower will be the clogging and the longer the service life. The effect of clogging for the 19-mm gravel after 6.2 years was more than that for the 38-mm gravel after 12.6 years. This supports the Ontario Ministry of Environment (Ontario Regulation 1998) requirement of using coarse gravel in drainage layers for MSW landfills with a D_{85} of gravel not less than 37 mm and a D_{10} of gravel not less than 19 mm.

The model confirmed the experimental findings that the leachate characteristics could change substantially after flowing through just a 0.57-m length of gravel layer and even more so after flowing through a 2.26-m length of gravel (mesocosms in series) because of biologically induced treatment in the gravel drainage layer. Thus, the leachate collected in a LCS (except at a very early time before the biofilm is established) does not represent the leachate entering the system for degradable compounds [volatile fatty acids (VFAs)] or species that may precipitate (e.g., calcium). Although this has advantages for leachate treatment, it also means that laboratory clogging studies conducted using leachate from a LCS in a landfill may underestimate the amount of clogging that could occur in the field. Likewise, the modeling studies (e.g., using BioClog) that were based on the leachate characteristics at the collection sump may significantly underestimate the clogging that would actually occur. It implies that to obtain a realistic estimate of clogging in the LCS of the MSW landfill, the characteristics of the leachate need to be selected to represent that entering the LCS and should not generally be that observed at sumps.

J. Geotech. Geoenviron. Eng. 2013.139:1022-1034.

Downloaded from ascelibrary.org by Queen's University Libraries on 06/19/14. Copyright ASCE. For personal use only; all rights reserved.

Conclusions

The original numerical model (BioClog) was enhanced to allow the modeling of the deposition of suspended particles within the saturated gravel drainage layers by the attachment of suspended particles (modeling suspended organic biomass with a diameter of 0.001 mm and suspended inorganic solids with a diameter of 0.002 mm) and by a deposition factor (considering the particle size range of suspended solids in real landfill leachate from 0.001 to 0.1 mm). This enhanced BioClog model was used to calculate the leachate characteristics and leachate-induced clogging of gravel within the saturated drainage layer of laboratory mesocosms. These mesocosms were run in full scale and permeated with real MSW landfill leachate (McIsaac 2007). Modeling was performed on mesocosms with 38- and 19-mm gravel, and for mesocosms with 38-mm gravel run-in series. Two sets of microbial kinetic rates were considered based on values calibrated for two independent sets of column tests (Case 1 for columns at 21°C and Case 2 for columns at 27°C).

Based on the predictive modeling of the mesocosm (using parameters established from others sources and not adjusted to fit the experimental data), the following conclusions were reached:

1. Allowing for the variability in the observed results for nominally identical mesocosms, the two sets of kinetic parameters generally bracketed the observed COD in the effluent over a 12-year period when experimental data were available. A lag period was initially predicted while the biofilm was developing, followed by a substantial decrease in COD values (based on reduced VFA concentrations).
2. Likewise, the model generally captured the changes in the calcium concentrations, although to the extent that it erred, it tended to overestimate the calcium concentrations in the effluent (i.e., underestimate the loss of calcium in the system).
3. There was substantial reduction in both COD and calcium concentrations after the leachate permeated a 0.56-m length of drainage gravel and a very substantial reduction after permeation through a 2.26-m length of drainage gravel in both the experimental observations and model predictions.
4. The calculated average porosities at both 6 and 12.6 years were in encouraging agreement with the measured values both for single mesocosms and up to four mesocosm in series. The predictions for the porosity of 38-mm gravel within mesocosms C03(04) from this paper were better than those from Cooke and Rowe (2008b) compared with the measured data, especially in the lower saturated drainage layer.
5. The model correctly predicted that the saturated drainage layer with 38-mm gravel at 12.6 years was more severely clogged than that at 6 years because of the increased mass loading over the extended period of permeation with leachate, and also correctly predicted a rise in leachate level into the initially unsaturated zone of the gravel as a result of clogging between 6 and 12.6 years.
6. The model correctly predicted that the drainage layer with 19-mm gravel would clog faster than that with 38-mm gravel, and that the clogging would cause a rise in leachate level in the 19-mm gravel layer but not in the 38-mm gravel layer after approximately 6 years, when both sets of mesocosms were permeated with same leachate.
7. The calculated geometric means of hydraulic conductivity over full saturated thickness from the influent end to the effluent end were in encouraging agreement with the measured values for the 38-mm gravel after 12 years of leachate permeation.

Downloaded from ascelibrary.org by Queen's University Libraries on 06/19/14. Copyright ASCE. For personal use only; all rights reserved.

Acknowledgments

This research was funded by a grant from the Natural Sciences and Engineering Research Council of Canada (NSERC). The authors are very grateful for the valuable discussions with Dr. Andrew Cooke.

References

Armstrong, M. D. (1998). "Laboratory program to study clogging in a leachate collection system." Masters thesis, Univ. of Western Ontario, London, ON, Canada.

Babcock, D. R. P. (2005). "An evaluation of model parameters for clogging of coarse drainage materials in landfill leachate collection systems." Masters thesis, Queen's Univ., Kingston, ON, Canada.

Bacas, B. M., Konietzky, H., Berini, J. C., and Sagaseta, C. (2011). "A new constitutive model for textured geomembrane/geotextile interfaces." *J. Geotextile Geomembr.*, 29(2), 137–148.

Bass, J. M. (1986)."Avoiding failure of leachate collection and cap drainage systems." *EPA-600/2-86-058*, EPA, Land Pollution Control Division, Hazardous Waste Engineering Research Laboratory, Cincinnati, OH.

Bennett, P. J., Longstaffe, F. J., and Rowe, R. K. (2000). "The stability of dolomite in landfill leachate collection systems." *Can. Geotech. J.*, 37(2), 371–378.

Bouchez, T., Munoz, M. L., Vessigaud, S., Bordier, C., Aran, C., and Duquennoi, C. (2003). "Clogging of MSW landfill leachate collection systems: Prediction methods and in situ diagnosis." *Proc., Sardinia 2003, 9th Int. Waste Management and Landfill Symp.*, CISA, Environmental Sanitary Engineering Centre, Cagliari, Italy (CD-ROM).

Brune, M., Ramke, H. G., Collins, H. J., and Hanert, H. H. (1991). "Incrustation processes in drainage systems of sanitary landfills." *Proc., Sardinia 91, 3rd Int. Landfill Symp.*, CISA, Environmental Sanitary Engineering Centre, Cagliari, Italy, 999–1035.

Cooke, A. J. (2007). "Modelling of clogging in landfill leachate collection systems." Ph.D. thesis, Univ. of Western Ontario, London, ON, Canada.

Cooke, A. J., and Rowe, R. K. (2008a). "2D modelling of clogging in landfill leachate collection systems." *Can. Geotech. J.*, 45(10), 1393–1409.

Cooke, A. J., and Rowe, R. K. (2008b). "Modelling landfill leachate induced clogging of field-scale test cells (mesocosms)." *Can. Geotech. J.*, 45(11), 1497–1513.

Cooke, A. J., Rowe, R. K., and Rittmann, B. E. (2005a). "Modelling species fate and porous media effects for landfill leachate flow." *Can. Geotech. J.*, 42(4), 1116–1132.

Cooke, A. J., Rowe, R. K., VanGulck, J. F., and Rittmann, B. E. (2005b). "Application of the BioClog model for landfill leachate clogging of gravel-packed columns." *Can. Geotech. J.*, 42(6), 1600–1614.

Chappel, M. J., Brachman, R. W. I., Take, W. A., and Rowe, R. K. (2012). "Large-scale quantification of wrinkles in a smooth, black, HDPE geomembrane." *J. Geotech. Geoenviron. Eng.*, 138(6), 671–679.

Craven, W., Townsend, T. G., Vogel, K., and Laux, S. (1999). "Field investigation of landfill leachate collection system clogging." *Pract. Period. Hazard. Toxic Radioact. Waste Manage.*, 3(1), 2–9.

Eid, H. T. (2011). "Shear strength of geosynthetic composite systems for design of landfill liner and cover slopes." *J. Geotextile Geomembr.*, 29(3), 335–344.

Fleming, I. R. (1999). "Biogeochemical processes and clogging of landfill leachate collection systems." Ph.D. thesis, Univ. of Western Ontario, London, ON, Canada.

Fleming, I. R., and Rowe, R. K. (2004). "Laboratory studies of clogging of landfill leachate collection and drainage systems." *Can. Geotech. J.*, 41(1), 134–153.

Fleming, I. R., Rowe, R. K., and Cullimore, D. R. (1999). "Field observations of clogging in a landfill leachate collection system." *Can. Geotech. J.*, 36(4), 685–707.

Fox, P. J., Ross, J. D., Sura, J. M., and Thiel, R. S. (2011). "Geomembrane damage due to static and cyclic shearing over compacted gravelly sand." *Geosynthetics Int.*, 16(5), 272–279.

Frind, E. O. (1988). "Solution of the advection-dispersion equation with free exit boundary." *Numer. Methods Partial Differ. Equ.*, 4(4), 301–313.

Gudina, S., and Brachman, R. W. I. (2011). "Geomembrane strains from wrinkle deformations." *J. Geotextile Geomembr.*, 29(2), 181–189.
Istok, J. (1989). *Groundwater modeling by the finite element method*, American Geophysical Union, Washington, DC.
Koerner, G. R., and Koerner, R. M. (1992). "Leachate flow rate behaviour through geotextile and soil filters and possible remediation methods." *J. Geotextile Geomembr.*, 11(4–6), 401–430.
Koerner, G. R., Koerner, R. M., and Martin, P. M. (1993). "Field performance of leachate collection systems and design implications." *Proc., of 31st Annual Int. Solid Waste Exposition*, Solid Waste Association of North America, Silver Spring, MD., 365–380.
Koerner, G. R., Koerner, R. M., and Martin, J. P. (1994). "Design of landfill leachate collection filters." *J. Geotech. Eng.*, 120(10), 1792–1801.
Levine, A. D., Cardoso, A. J., Nayak, B., Rhea, L. R., Dodge, B. M., and Harwood, V. J. (2005). "Assessment of biogeochemical deposits in landfill leachate drainage systems." *Project Final Rep.*, Center for Solid and Hazardous Waste Management, Gainesville, FL.
Maliva, R. G., et al. (2000). "Unusual calcite stromatolites and pisoids from a landfill leachate collection system." *Geology*, 28(10), 931–934.
McBean, E. A., Mosher, F. R., and Rovers, F. A. (1993). "Reliability-based design for leachate collection systems." *Proc. of Sardinia 93, 3rd Int. Landfill Symp.*, Santa Margherita di Pula, Cagliari, Italy, CISA, Environmental Sanitary Engineering Centre, Cagliari, Italy, 433–441.
McIsaac, R. (2007). "An experimental investigation of clogging in landfill leachate collection systems." Ph.D. thesis, Univ. of Western Ontario, London, ON, Canada.
McIsaac, R., and Rowe, R. K. (2006). "Effect of filter-separators on the clogging of leachate collection systems." *Can. Geotech. J.*, 43(7), 674–693.
McIsaac, R., and Rowe, R. K. (2007). "Clogging of gravel drainage layers permeated with landfill leachate." *J. Geotech. Geoenviron. Eng.*, 133(8), 1026–1039.
Metcalf and Eddy, Inc. (1991). *Wastewater engineering: Treatment, disposal, and reuse*, 3rd Ed., McGraw Hill, New York.
Ontario Regulation. (1998). "Environmental Protection Act Ontario." *Ontario Regulation 232/98, PIBS 3651E,* Ontario Ministry of the Environment, Toronto.
Padilla, F., Secretan, Y., and Leclerc, M. (1997). "On open boundaries in the finite element approximation of two-dimensional advection-diffusion flows." *Int. J. Numer. Methods Eng.*, 40(13), 2493–2516.
Pavlostathis, S. G., and Giraldo-Gomez, E. (1991). "Kinestics of anaerobic treatment: A critical review." *Crit. Rev. Environ. Control*, 21(5-6), 411–490.
Rayhani, M. T., Rowe, R. K., Brachman, R. W. I., Take, W. A., and Siemens, G. (2011). "Factors affecting GCL hydration under isothermal conditions." *J. Geotextile Geomembr.*, 29(6), 525–533.
Rittman, B. E. (1982). "The effect of shear stress on biofilm loss rate." *Biotechnol. Bioeng.*, 24(2), 501–506.
Rittmann, B. E., and Brunner, C. M. (1984). "The non-steady state biofilm process for advanced organics removal." *J. Water Pollut. Control Fed.*, 56(7), 874–880.
Rittmann, B. E., and McCarty, P. L. (1981). "Substrate flux into biofilms of any thickness." *J. Environ. Eng.*, 107(4), 831–849.
Rittmann, B. E., and Snoeyink, V. L. (1984). "Achieving biologically stable drinking water." *J. Am. Water Works Assoc.*, 76(10), 106–114.
Rowe, R. K. (1998). "From the past to the future of landfill engineering through case histories." *Proc., 4th Int. Conf. on Case Histories in Geotechnical Engineering*, Univ. of Missouri-Rolla, Rolla, MO, 145–166.
Rowe, R. K. (2005). "Long-term performance of contaminant barrier systems. 45th Rankine Lecture." *Geotechnique*, 55(9), 631–678.
Rowe, R. K. (2011). "Systems engineering the design and operations of municipal solid waste landfills to minimize leakage of contaminants to groundwater." *Geosynthetics Int.*, 18(6), 391–404.
Rowe, R. K. (2012a). "Short and long-term leakage through composite liners." *Can. Geotech. J.*, 49(2), 141–169.
Rowe, R. K. (2012b). "Third Indian Geotechnical Society: Ferroco Terzaghi oration design and construction of barrier systems to minimize environmental impacts due to municipal solid waste leachate and gas." *Indian Geotech. J.*, 42(4), 223–256.
Rowe, R. K., and Babcock, D. (2007). "Modelling the clogging of coarse gravel and tire shreds in column tests." *Can. Geotech. J.*, 44(11), 1273–1285.
Rowe, R. K., Chappel, M. J., Brachman, R. W. I., and Take, W. A. (2012). "A field study of wrinkles in a geomembrane at a composite liner test site." *Can. Geotech. J.*, 49(10), 1196–1211.
Rowe, R. K., Quigley, R. M., Brachman, R. W. I., and Booker, J. R. (2004). *Barrier systems for waste disposal facilities.* Taylor & Francis Books Ltd, London.
Rowe, R. K., VanGulck, J. F., and Millward, S. (2002). "Biologically induced clogging of a granular media permeated with synthetic leachate." *J. Environ. Eng. Sci.*, 1(2), 135–156.
Taylor, S. W., and Jaffe, P. R. (1990). "Biofilm growth and the related changes in the physical properties of a porous medium, Part 3: Dispersivity and model verification." *Water Resour. Res.*, 26(9), 2153–2159.
Tien, C., and Ramarao, B. V. (2007). *Granular filtration of aerosols and hydrosols*, Elsevier, Oxford, U.K.
VanGulck, J. F. (2003). "Biodegradation and clogging in gravel size material." Ph.D. thesis, Queen's Univ., Kingston, ON, Canada.
VanGulck, J. F., and Rowe, R. K. (2004a). "Evolution of clog formation with time in columns permeated with synthetic landfill leachate." *J. Contam. Hydrol.*, 75(1–2), 115–135.
VanGulck, J. F., and Rowe, R. K. (2004b). "Influence of landfill leachate suspended solids on clog (biorock) formation." *Waste Manag.*, 24(7), 723–738.
VanGulck, J. F., and Rowe, R. K. (2008). "Parameter estimation for modelling clogging of granular medium permeated with leachate." *Can. Geotech. J.*, 45(6), 812–823.
VanGulck, J. F., Rowe, R. K., Rittmann, B. E., and Cooke, A. J. (2003). "Predicting biogeochemical calcium precipitation in landfill leachate collection systems." *Biodegradation*, 14(5), 331–346.
Wilson, E. J. and Geankoplis, C. J. (1966). "Liquid mass transfer at very low Reynolds numbers in packed beds." *Industrial and Engineering Chemistry Fundamentals*, 5(1), 9–14.
Yu, J., and Pinder, K. L. (1994). "Effective diffusivities of volatile fatty acids in methanogenic biofilms." *Bioresour. Technol.*, 48(2), 155–161.
Yu, Y. (2012). "Modelling MSW leachate characteristics and clogging." Ph.D. thesis. Dept. of Civil Engineering, Queen's Univ., Kingston ON, Canada.
Yu, Y., and Rowe, R. K. (2012a). "Modelling leachate-induced clogging of porous media." *Can. Geotech. J.*, 49(8), 877–890.
Yu, Y., and Rowe, R. K. (2012b). "Improved solutions for porosity and specific surface of a uniform porous medium with attached film." *J. Environ. Eng.*, 138(4), 436–445.

Downloaded from ascelibrary.org by Queen's University Libraries on 06/19/14. Copyright ASCE. For personal use only; all rights reserved.

J. Geotech. Geoenviron. Eng. 2013.139:1022-1034.